RFQ MATCH BY ADIABATIC BEAM COMPRESSION*

Reinard Becker and Norbert Zoubek

Institut für Angewandte Physik der Universität Frankfurt,
Robert-Mayer-Straße 2-4, D-6000 Frankfurt am Main 1, FRG

Abstract

The physical and mathematical similarity of matching either electrons into high density Brillouin flow or ions into an RFQ channel is demonstrated by transforming the pertinent differential equations to the same normalized equation. By investigating the influence of different kinds of build-up of the focusing force it is shown, that the axial gradient of this force is most important for the beam behaviour in the transition region, causing inevitably an adiabatic beam compression. The entrance conditions for the beam to be matched can be expressed in a unique way by the compression taking place between the electrostatic waist of the spreading beam and of the focused beam. Results are given for linear, sin and sin² build-up and all relevant parameters, covering most of the practical cases of beam injection. These general results are used to start PARMTEQ calculations, which agree excellently and give some insight for an optimum length of the transition region.

1. Introduction

Electron beams can be focused by superconducting solenoids to current densities in the 10^3 to 10^4 A/cm² range[1]. Since high intensity electron guns must utilize impregnated cathodes with current density ratings of a few A/cm², considerable beam compression becomes necessary, of which only a factor of 100 can be done electrostatically. On the other hand, such solenoidal fields cannot be made with a field build-up short compared to the beam spread behaviour, therefore a correct injection of a high intensity electron beam into high density Brillouin flow utilizes the inevitable ramp of the magnetic field for an additional adiabatic magnetic beam compression[2]. As may be seen from fig. 1, the compression grows with increasing transition length. Most favorable for matching is the decreasing entrance slope of the beam at high compression rates.

The same situation is met with the matching problem of a high intensity ion beam into the high density focused beam inside of an RFQ channel. Here, a certain build-up length of the focusing force becomes mandatory to allow for the adiabatic transition from the axisymmetric DC ion beam to the transversely RF focused beam of the RFQ[3].

Both matching problems will be solved in the same way, by transforming the appropriate differential equations for focusing - namely the paraxial ray equation in the electron case and the KV envelope equation for the RFQ ion focusing - into the same normalized differential equation. The normalization is based on the equilibrium focused beam and therefore leaves only one free parameter - cathode flux for the electron beam or the ratio of emittance to acceptance in the RFQ case. This differential equation is then solved by numerical integration, starting with the well defined focused beam and taking into account 3 different shapes for the build-up of the focusing force, linear, sine and square of sine. To come free from the normalization factors, the results are given in terms of the beam compression taking place in the transition region.
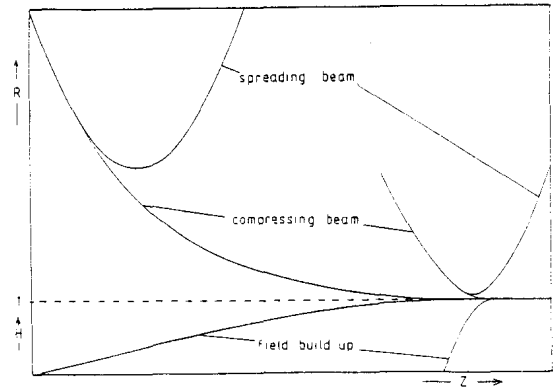
Fig. 1 Sine shaped build-up of the focusing force H(Z) for 2 different transition lengths, corresponding beam envelopes and beam spreading curves for the same injection conditions

2. Normalization of the Differential Equations for Focusing

a) The Paraxial Ray Equation

Busch's theorem being equivalent to the conservation of the canonical angular momentum can be given in the paraxial approximation as

$$\dot{\varphi} = \frac{\eta}{2} B_z \left(1 - \frac{B_c r_c^2}{B_z r^2}\right) \qquad (1)$$

Using this and the homogeneous radial space charge of the beam by

$$E_r = - \frac{I}{2\pi\varepsilon_0 v_z \cdot r} \qquad (2)$$

the radial force equation for the outermost electron of a laminar beam has the form

$$\ddot{r} = \frac{\eta I}{2\pi\varepsilon_0 v_z \cdot r} - \frac{\eta^2}{4} B_z^2 r + \frac{\eta^4}{4} \frac{B_c^2 r_c^4}{r^3} \qquad (3)$$

which is known as the "Paraxial Ray Equation"[4].

There exists a solution, called Brillouin flow, where $\ddot{r} = 0$ for a certain set of $r = r_0$, $B_z = B_0$:

$$\frac{I}{\pi r_0^2} = j_B = \varepsilon_0 v_z \frac{\eta}{2} B_0^2 \{1 - K^2\} \qquad (4)$$

where $K = B_c r_c^2 / B_0 r_0^2$ is the flux compression. With this balance condition of eq. (4), the paraxial ray equation eq. (3) may be written as

$$\frac{\ddot{r}}{\frac{\eta^2}{4} B_0} = \frac{1 - K^2}{\frac{r}{r_0}} - \left(\frac{B_z}{B_0}\right)^2 \cdot \frac{r}{r_0} + \frac{K^2}{\left(\frac{r}{r_0}\right)^3} \qquad (5)$$

which is normalized by

$$R = \frac{r}{r_0} , \quad Z = \frac{\eta}{2} B_0 \cdot t = \frac{\eta}{2} B_0 \cdot \frac{z}{v_z}, \quad H = \frac{B_z}{B_0} \qquad (6)$$

to

$$\frac{d^2 R}{dZ^2} = \frac{1 - K^2}{R} - H^2 R + \frac{K^2}{R^3} \qquad (7)$$

In this equation the beam radius has to be taken in units of the Brillouin radius, and the axial coordinate is measured by the beam gyration with the Larmor frequency $\eta/2 \cdot B_0$.

By $H = H(Z)$ any axial variation of the focusing force can be introduced to study the beam behaviour. The only free parameter in this formulation is the flux compression factor K, which reduces drastically the focused current density (eq. (4)), if the cathode field B_C is not made small with respect to the beam compression taking place.

b) The KV Envelope Equation

The mean beam radius a of an ion beam focused in a RFQ is given by the KV envelope equation[5],[6].

$$a'' = \frac{K_p}{a} - \kappa(z)a + \frac{\varepsilon^2}{a^3} \qquad (8)$$

Hereby it is assumed that the emittance ε is equal in both transverse directions. $\kappa(z)$ represents the average focusing force, which is increasing in the matching section. The constant K_p represents the generalized perveance:

$$K_p = \frac{I}{I_o} \frac{2}{\beta^3 \gamma^3}, \text{ where } I_o = \frac{4\pi\varepsilon_o mc^3}{e} \qquad (9)$$

For the matched beam the beam radius remains the same for constant focusing force:

$$a'' = 0, \quad a = a_o, \quad \kappa = \kappa_o \qquad (10)$$

In this case we get from eq. (8):

$$K_p = \kappa_o a_o^2 - \frac{\varepsilon^2}{a_o^3}, \qquad (11)$$

which is equivalent to Reiser's current limit[5]:

$$I = \frac{I_o}{2} \beta^3 \gamma^3 \frac{\sigma_o}{\beta\lambda} \alpha[1 - (\frac{\varepsilon}{\alpha})^2], \qquad (12)$$

where $\alpha = a_o^2 \cdot \sqrt{\kappa_o}$ is defined as the acceptance, which causes the current to be proportional to the beam area.

Hence the introduction of a limiting current density would be more physical and corresponds to the Brillouin density (eq. (4)). In the RFQ case we get

$$j_{lim} = \varepsilon_o \frac{m}{2\pi^2 e} v_z (\sigma_o\omega)^2 \gamma^3 [1 - (\frac{\varepsilon}{\alpha})^2], \quad (13)$$

where ω is the operating frequency.

Replacing the generalized perveance in eq. (8) by the balance condition (eq. (11)) the envelope equation now reads:

$$\frac{a''}{\kappa_o} = \frac{1 - (\frac{\varepsilon}{\alpha})^2}{\frac{a}{a_o}} - \frac{\kappa(z)}{\kappa_o} \frac{a}{a_o} + \frac{(\frac{\varepsilon}{\alpha})^2}{\frac{a^3}{a_o^3}} \qquad (14)$$

We abbreviate

$$H^2 = \frac{\kappa(z)}{\kappa_o}, \quad K = \frac{\varepsilon}{\alpha} \qquad (15)$$

and insert new normalized coordinates

$$R = \frac{a}{a_o}, \quad Z = \sqrt{\kappa_o}z = \sigma_o\frac{z}{\beta\lambda} \qquad (16)$$

to obtain

$$\frac{d^2R}{dZ^2} = \frac{1 - K^2}{R} - H^2R + \frac{K^2}{R^3}, \qquad (17)$$

which is exactly the normalized differential equation for electron focusing (eq. (7)), where we have given the same constant K to the emittance to acceptance ratio as for the flux compression before. Now the axial coordinate is measured in terms of $\beta\lambda$ - the spatial periodicity of the RF field - times the phase advance σ_o.

3. Numerical Integration and Results

The normalized differential equation for the beam boundary (eqs. (7) and (17)) now can be solved by a standard Runge-Kutta subroutine for

any given value of K (eqs. (4) and (15)) and a prescribed build-up of the focusing force $H(Z)$. This build-up may be characterized by its shape (e. g. linear, sine or square of sine in this investigation) and by its transition length. For comparing different shapes of $H(Z)$ we define the transition length as the reciprocal of the maximum slope of $H(Z)$. Hence the 3 investigated shapes of $H(Z)$

$$
H(Z) =
\begin{matrix}
I & \frac{Z}{\Lambda} & & 0 < Z < \Lambda \\
II & \sin\frac{Z}{\Lambda} & \text{for} & 0 < Z < \frac{\pi}{2}\Lambda \\
III & \sin^2\frac{Z}{\Lambda} & & 0 < Z < \frac{\pi}{2}\Lambda
\end{matrix}
\qquad (18)
$$

have all the maximum slope $1/\Lambda$ and therefore the same transition length Λ.

Since the beam is well defined for $H(Z) = 1$, namely $R = 1$, $R' = 0$, $R'' = 0$, we start to integrate at $Z = \frac{\pi}{2} \cdot \Lambda$ and decrement Z to 0. The resulting values of $R_o = R(Z=0)$ and $R_o' = R'(Z=0)$ define the injection conditions for the beam to be matched. However, due to the normalized Z-axis, the interpretation of the slope is difficult, even more in making a match with measured data of the spreading beam. Known in general are the position and the diameter of the waist for the spreading beam. Therefore the position and the diameter of the waist should be adjusted in such way that correct entrance conditions R_o and R_o' occure for injection.

To facilitate this procedure we calculate the beam spreading behaviour for the entrance conditions obtained. The resulting crossover radius R_{min} then can be determined from the compression

$$R_{min} = \sqrt{\kappa_m}, \qquad (19)$$

whereas the electrostatic compression

$$\kappa_e = (\frac{R_o}{R_{min}})^2 \qquad (20)$$

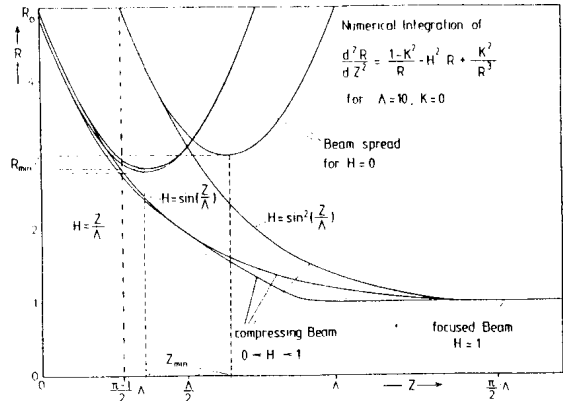characterizes the axial position of the waist with respect to the focusing force build-up.

Fig. 2 Beam envelopes for linear, sin and sin² shaped ramp of the field with a transition length of 10 and corresponding beam spreading

In fig. 2 we compare curves of the compressing beam together with curves for beam spread obtained with the same injection conditions for the 3 field build-up shapes (eq. (18)), a normalized transition length of $\Lambda = 10$ and $K = 0$. We want to point out that the linear and the sine shaped field increases need nearly the same injection conditions; where linear and sine shape differ from each other, the beam seems to adjust adiabatically. Even more surprising is the fact, that square of sine gives almost identical results,

with the difference, however, that the axial
position of the waist is about $(\pi-1)*\Lambda/2$ closer
to the field ramp. Exactly this is the Z-axis
intersection of a tangent to $\sin^2$ in the point
of maximum slope.

The interpretation of the influence of different
field shapes therefore is that the maximum gra-
dient of the focusing force is mainly respon-
sible for the beam behaviour. On variations of
$H(Z)$ in the high field region, the beam reacts
by adiabatic compression, whereas variations at
low field seem to be unimportant. The latter is
not true for very long transition regions, which
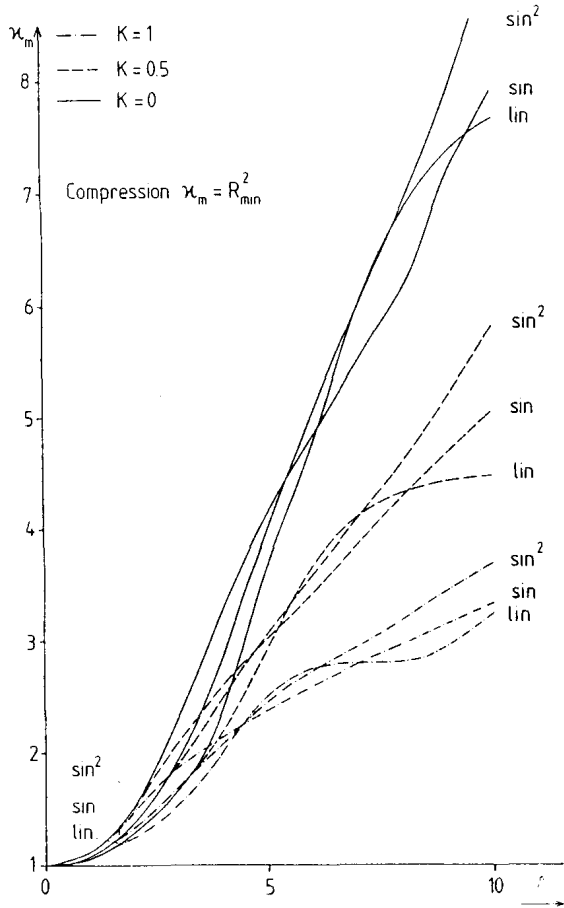are not considered here.

Fig. 3   Compression of the beam envelope by a
          tapered increase of the focusing field
          as compared to the waist of the sprea-
          ding beam

For different transition lengths Λ up to 10
and values of K of 0, 0.5, 1 fig. 3 shows the
"magnetic" compression, as defined by eq. (19).
For short Λ there is nearly no K-dependence, but
for $\Lambda > 4$ the shape dependence seems to die out
at the expense of a K-dependence. For larger va-
lues of Λ the ratio κ_m/Λ becomes the same and
nearly constant for linear and sine shape. A
fairly good approximation for $K < 0.7$, $\Lambda > 3$ is

$$\frac{\kappa_m}{\Lambda} \cong 0.775 \ (1 - K) \qquad (21)$$

which can be used for an estimate of the cross-
over radius.

For the electrostatic compression, which the
spreading beam should show within the transition
region, the parameter dependence is given by
fig. 4. Again we see no dependence for small Λ,
but only K-dependence for $\Lambda > 2$. For small K
(< 0.7) but large Λ there is $\kappa_e = 3.15(1-0.36\ K^2)$.
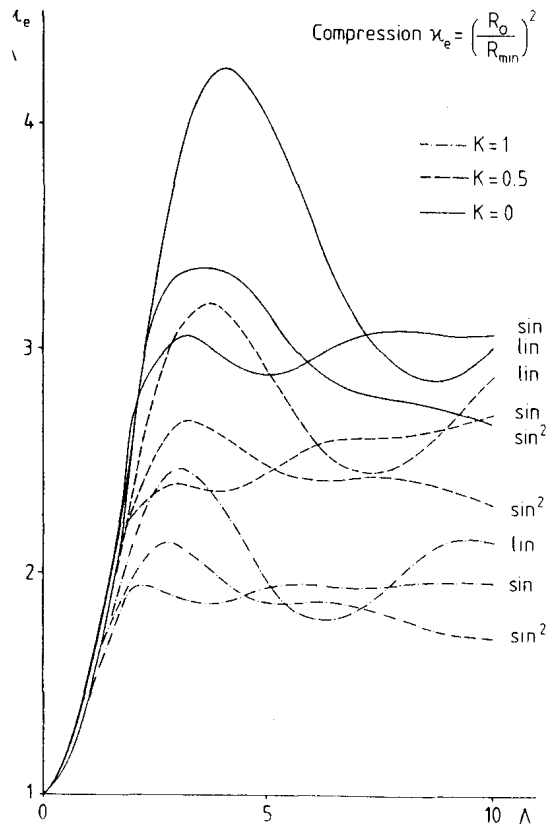

Fig. 4   Compression necessary for the spreading
          beam between start of the field build-up
          and crossover

This allows to give a simple rule for the position of
the electrostatic waist with respect to the field
build-up: At the intersection of the tangent to
the field shape curve in its steepest point with
the abscissa, the injected beam should have $\sqrt{3.15}$
$\cong 1.8$ times the crossover radius for $K = 0$ etc.

The results presented here now can be used
for both, injection of electrons into Brillouin
flow and matching an ion beam to an RFQ channel,
by using the appropriate normalization formulae
for the axial coordinate eqs. (6) and (16). In
the electron case, however, there may also exist
the situation, where the cathode flux term K va-
nishes with the focusing field being turned off.
Then the beam spread behaviour for $K \neq 0$ is dif-
ferent and these results cannot be used, although
the differences are small.

4. Calculations with the PARMTEC-Code

The results of the smooth approximation theo-
ry (chapter three) have been tested by PARMTEQ-
calculations. All computations have been carried
out for a matching section followed by an unmo-
dulated RFQ-channel with a length of 10 $\beta\lambda$. For
a beam of α-particles with 10 keV injection ener-
gy, 4 mm aperture radius and an operating fre-
quency f = 18 MHz the normalized transition length
Λ equals 1.05, if the actual transition length
is 1 $\beta\lambda$ and $\sigma_o = \pi/3$ (60°)(eq. (16)).

The input phase space ellipse parameters A,B,
ϵ in both transverse directions are equal and
calculated by

$$B = \frac{(a_o R_o)^2}{\epsilon} \ , \quad A = \frac{\tan^{-1}(\frac{a_o \sigma_o}{\beta\lambda} R_o')}{\sqrt{\epsilon/(a_o R_o)}} \qquad (22)$$

In the transverse directions the particle di-
stribution is of the KV-type, in the longitudi-

nal direction it is homogeneous.

In fig. 5 the smooth theory envelope by inte-
gration of eq. (17) and the x,y-envelopes from
PARMTEQ are shown. The "true" oscillating enve-
lopes are well presented by the "smooth" enve-
lope, but the PARMTEQ calculations give additio-
nal informations about the beam losses. At the
entrance of the matching section only the emit-
tance dominated beam (K = 1) is close enough to
the axis to avoid losses on the matching elec-
trodes. In contrast, the space charge dominated
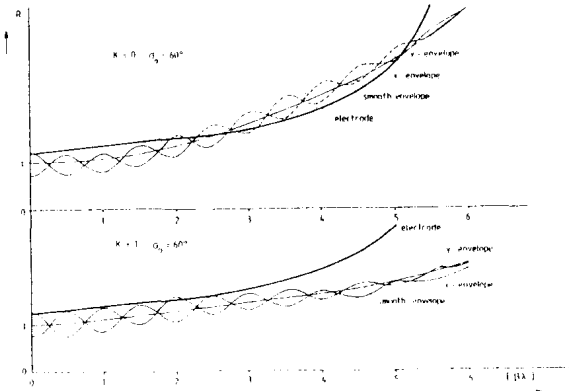beam (K = 0) would partly impinge on the elec-
trodes.

Fig. 5 A comparison of beam envelopes as cal-
culated with the KV smooth approxima-
tion theory and with PARMTEQ together
with the location of the electrode

In fig. 6 the transmission rate as a func-
tion of the matching section length is presen-
ted for different phase advances σ_0 for a li-
near taper. (As expected from the "smooth" re-
sults, this situation does not change, if in-
stead of a linear, a sinusoidal taper is used).
The transmission without a matcher is less than
50 %, going down for increasing σ_0, because the
DC-axisymmetric beam is not directly matched
to the transversely RF-focused beam. For all
cases the transmission is increasing conside-
rably by small matching lengths of 1 $\beta\lambda$. The
emittance dominated beams (K = 1) show further
(less steep) increase for longer matchers,
whereas the space charge dominated beams have
a maximum of transmission for matchers of
lengths 1 to 2 $\beta\lambda$. This maximum of transmission
is decreasing for higher values of σ_0, but the
total current, which is proportional to trans-
mission times square of σ_0, is still increasing.
To explain this, we assume that the distance
between the RFQ electrodes is increasing accor-
dingly with the beam radius. Then the mean beam
radius becomes proportional to the aperture ra-
dius and the focusing force in eq. (17) propor-
tional to $1/R^3$. If an emittance dominated beam
blows up, the ratio of the beam spreading force
to the focusing force remains constant, while
for a space charge dominated beam the spreading
force at larger values of R is much stronger
than the focusing force.

Also there is no remarkable difference in
using matching sections of integer or non inte-
ger multiples of $\beta\lambda$.[7]

Finally we want to point out that the trans-
mission calculations may be pessimistic. Every
quadrupole shows end fringe fields, which may
be used as matching sections, but do not give
rise to particle losses. The optimum length for
the matching section therefore could be slight-
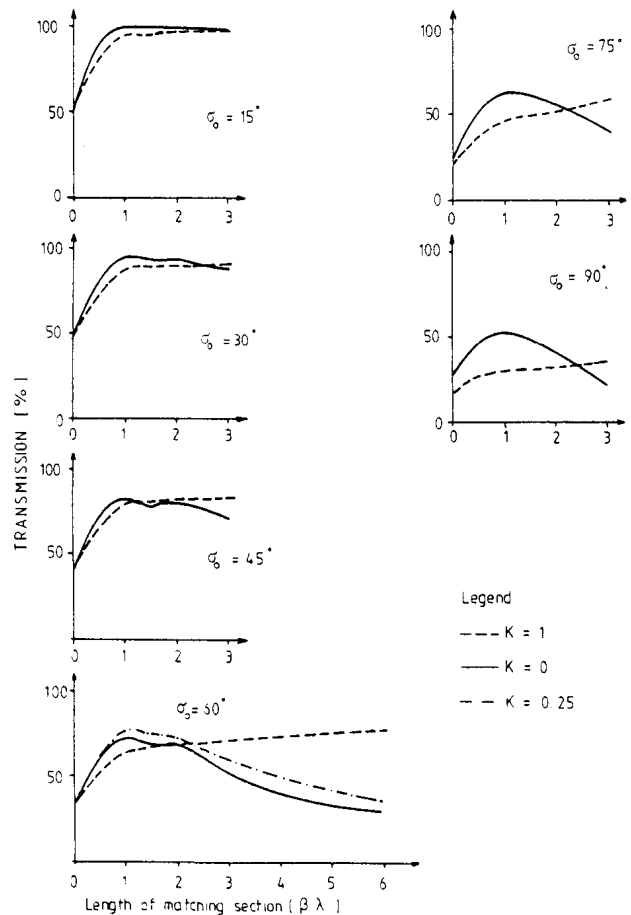ly higher for the space charge dominated beam
than indicated by fig. 6.

Fig. 6 Beam transmission through a 10 $\beta\lambda$ long
RFQ in dependence of the matcher length,
the phase advance σ_0, and the emittance
to acceptance ratio K.

5. Summary

The matching-in problem for a RFQ has been
solved in a general way by integrating the nor-
malized KV-smooth approximation envelope equa-
tion. The results are given in such a way as
to allow an easy decision on the diameter and
the axial position of the electrostatic waist
with respect to the ramp of the field build-up
in the matcher section. It has been demonstra-
ted that the gradient of the focusing field de-
termines the entrance conditions. PARMTEQ cal-
culations are in excellent agreement with these
results, but give information on beam losses:
Emittance dominated beams may have complete
transmission for very long matcher sections,
space charge dominated beams never have full
transmission, but require matcher sections with
a length of 1 to 2 $\beta\lambda$ only.

6. References

[1] II. EBIS-Workshop, Saclay-Orsay 1981, J. Aria-
ner, M. Olivier (Edts.)
[2] K. Amboss, Studies of a magnetically compres-
sed electron beam, IEEE-ED 16, 11 (1969) 897
[3] N. Tokuda, S. Yamada, New formulation of the
RFQ matching section, Los Alamos, LA-9234-C
(1982) 313
[4] P.T. Kirstein, G.S. Kino, W.E. Waters, Space
charge flow, Mc Graw Hill: 1967.
[5] M. Reiser, Part. Acc., Vol. 8 (1978) 167
[6] P. Junior, Part. Acc., Vol. 13 (1983) 231
[7] K.R. Crandall, Proposal for a new radial mat-
ching section for RFQ linacs. Los Alamos, Of-
fice memorandum AT1 (1983)